New Injection Kicker Magnets for the Daresbury SRS

J A Clarke and J N Corlett*
SERC Daresbury Laboratory, Daresbury, Warrington WA4 4AD, UK
*Now at Lawrence Berkeley Laboratory, University of California, Berkeley CA94720, USA

Abstract

New injection kicker magnets for the Daresbury SRS storage ring are described. These are designed for reduced physical dimensions and broadband impedance and to produce a peak integrated field of 6 mT-m from a half sinusoidal waveform of 2 μs duration. A simple, cost effective design is discussed, optimised by a commercially available software package PE2D [1]. Measurements of the magnetic properties and of the longitudinal broadband impedance are presented.

1. INTRODUCTION

Replacement injection kicker magnets are required in the Daresbury SRS storage ring to facilitate the inclusion of a new 6T superconducting wiggler magnet into the lattice [2]. The location of this insertion device results in a movement of the lumped sextupole magnets [3], and this in turn requires new, compact injection kicker magnets to allow the inclusion of a sextupole magnet adjacent to the kicker. As well as the reduced physical length, the design of the new kicker magnets was aimed to reduce the broadband impedance of the kickers, which have been identified as a significant contribution to the total impedance of the storage ring [4]. All three kicker magnets have been replaced.

The injection process requires an angular deflection of approximately 3 mrad from the kicker magnets, corresponding to an integrated field of 6 mT-m at the injection energy of 600 MeV. A half sine wave current pulse of 2 μs duration is used to drive the magnet at a maximum of 10 Hz repetition frequency. The physical length of approximately 0.5 m flange to flange is determined by the requirement to accommodate a sextupole magnet in the same straight section. A magnetic length of 0.425 m was assumed for the design, resulting in a peak field requirement of 14 mT.

To reduce the complexity, a design was developed which uses a simple arrangement of two conductors running parallel to the beam. Driven by a power supply, operating with a single thyratron, capable of producing a peak current of approximately 8 kA. Beam-stay-clear and radiation shadowing requirements limit the spacing of the conductors to a minimum of 140 mm. For acceptable incoherent beam displacement, a field variation of <2% over ±10 mm from the axis was specified.

The desired magnetic field of the pulsed magnet is reduced from that of a similar magnet in free space by the effects of currents induced on the vacuum vessel inner walls. These currents are created as a result of the time varying fields of the driven conductors and produce a magnetic field acting against the primary field. Since the drive current is limited, this represents the most important limitation in the design of the compact pulsed magnets.

2. ANALYTICAL STUDIES

In order to estimate the magnitude of the effect of the induced wall currents, an analytical model of a TEM mode on a twin wire transmission line in a cylindrical vessel was studied. Figure 1 shows the geometry. To simplify calculations all metal surfaces were assumed to be perfectly conducting. The resulting magnetic field strength at the centre of the vessel as a function of vessel inner radius is shown in figure 2. For the given conductor arrangement a vessel of radius 100 mm (approximately twice the typical SRS vacuum chamber dimension) reduces the magnetic field strength on axis by a factor 0.6 compared to that given in the limit of an infinitely large radius.

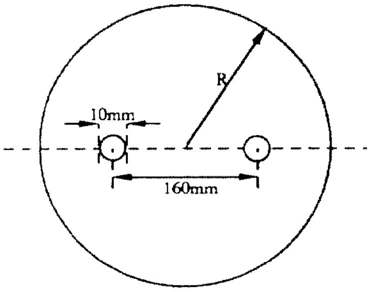

Figure 1. Geometry of the transmission line model

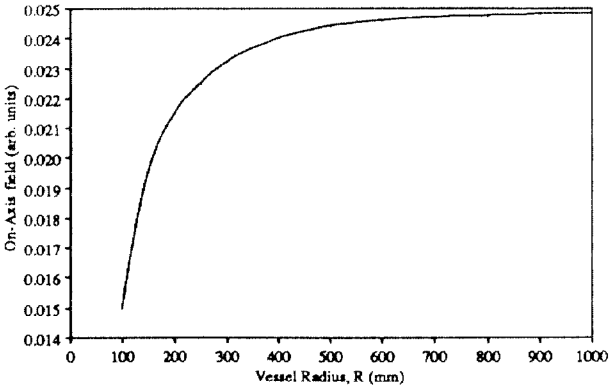

Figure 2. On-axis magnetic field as a function of vessel radius

Field uniformity near the axis is poor for this model, rectangular section conductors were chosen to improve the field quality. The analytic TEM mode transmission line model does not readily allow inclusion of arbitrary conductor sections, or of skin depth effects, and development proceeded by the use of finite element software.

3. FINITE ELEMENT ANALYSIS

A more rigorous analysis than the resonant TEM mode solution is required to model the low frequency response of the real kicker magnet with arbitrary geometries. The 2-dimensional finite element electromagnetic design code PE2D has been used to model various kicker magnet designs. Although the code does not solve all of Maxwell's equations (it does not include displacement current terms) the results are acceptable for this 'quasi-static' case where the wavelengths involved are much greater than the model size.

A model similar to that of figure 1 predicts an attenuation of 0.67 with a vessel of inner radius 100 mm compared to free space, which is in reasonable agreement with the transmission line TEM mode model, and includes skin depth effects. Figure 3 shows a quarter section of the final magnet design, with magnetic equipotential lines, modelled with PE2D. Rectangular conductors spaced 140 mm apart and of height 60 mm, width 5 mm, are housed in a vessel of inner radius 115 mm. A sinusoidal drive current is used, corresponding to the 2.2 μs half sine wave pulse (i.e. 227 kHz). In order to model skin depth effects all conducting surfaces were created with a mesh layer of at least 3 skin depths and 3 nodes per skin depth. The conductivity of the copper conductors was taken to be $5.8\times10^{7}\ \Omega^{-1}$m and the stainless steel vessel $1.0\times10^{7}\ \Omega^{-1}$m.

A peak field strength of 2.85 mT/kA peak drive current was predicted from the model, corresponding to a drive current requirement of 5 kA. Field variation of 2% over ±10 mm horizontally from the central axis was estimated and field penetration through the vessel walls was negligible. The inductance was estimated at 0.21 μH, neglecting end effects and the contribution from the electrical feedthrough.

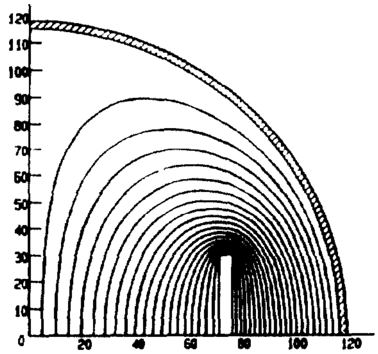

Figure 3. PE2D model of a quarter kicker including magnetic equipotentials (dimensions in mm)

4. MAGNETIC MEASUREMENTS

Measurements of the magnetic field of the kickers were made using inductive loops placed in the field. The voltage induced across the ends of the loop is determined by the rate of change of flux linking the loop. Integrating the voltage output allows calculation of the average magnetic field enclosed by the loop whose dimensions are known. Integration is readily achieved using a simple LC integrator circuit with time constant greater than that of the pulse being measured.

Two types of inductive loop were used: a long single turn which passed along the whole length of the magnetic field, and a small single turn circular loop. The long loop was used to provide a direct ∫B.dl measurement through the magnet. This loop was mounted along the central axis and was fabricated by etching a double sided circuit board to produce parallel strips of conductor 2 mm high on opposite sides of the board. The separation of the conductors is determined by the board thickness of 3.175 mm, over which PE2D predicts negligible field variation. The small circular loop was wound from a length of copper wire, and mounted on a long tufnol rod. An adjustable positioning system was used to locate the loop at various points inside the kicker, to measure the field locally and to allow a scan of the field profile through the magnet. Figure 4 shows the magnetic field strength along the axis of the kicker at 6 kA peak drive current.

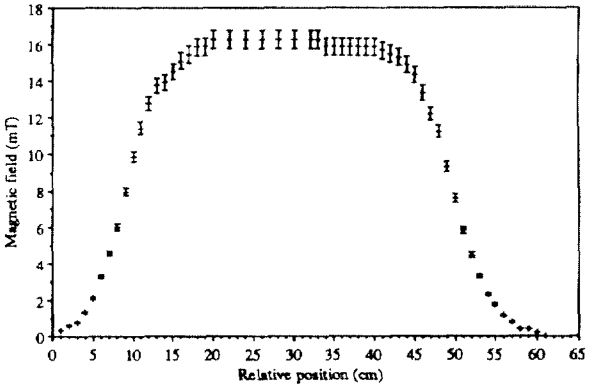

Figure 4. Magnetic field along axis at 6 kA

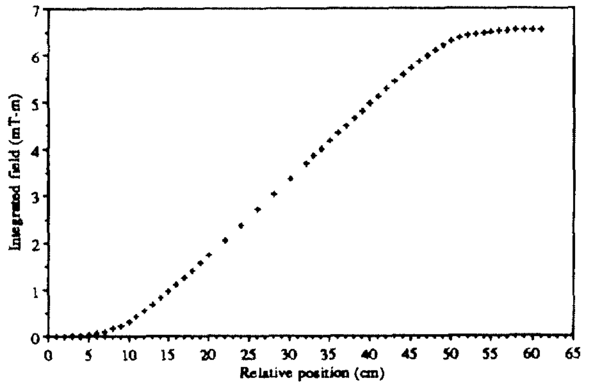

Figure 5. Integrated magnetic field along the axis at 6 kA

The measured maximum field strength of 16.25 mT is 5% lower than computed using PE2D, which may in part be due to the use of a steady state drive current in the computer model, but remains within the estimated error of 6% for this measurement. The integrated field (derived from the data of figure 4) is shown in figure 5 and the horizontal displacement of the electron beam, determined from the double integral, is shown in figure 6. At 6 kA drive current an integrated field of 6.5 mT-m corresponding to an exit angle of 3.25 mrad is found.

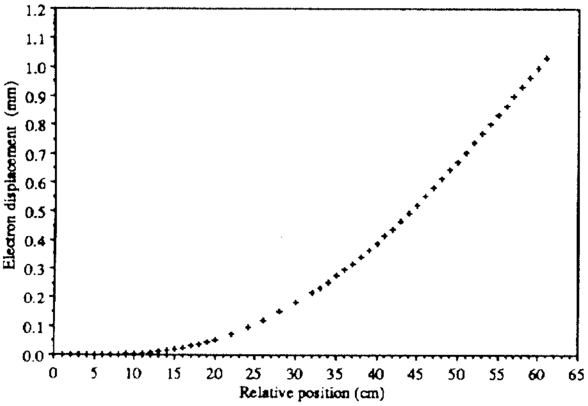

Figure 6. Electron displacement through the kicker at 6 kA

Measured quadrupole and sextupole components of 6.2 T/m and 3 T/m^2 are respectively 10% higher and 18% lower than computed by PE2D. Integrated field measurements, using the long loop, as a function of drive current are shown in figure 7. A drive current of 5.7 kA is required to achieve the specified integrated field of 6 mT-m. The measured dipole magnetic length of 0.39 m is reduced by 8% from the physical length of the conductors, due to end effects.

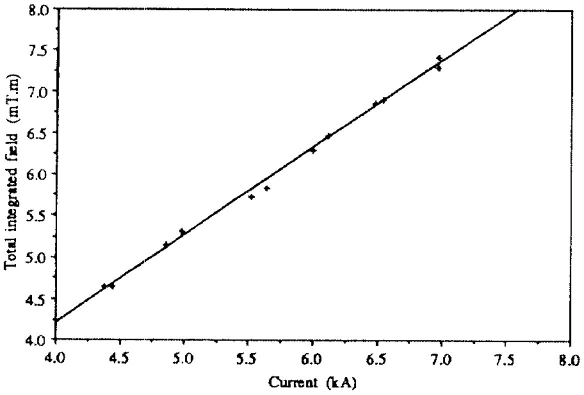

Figure 7. Total integrated field as a function of drive current

5. IMPEDANCE MEASUREMENTS

Computations using the MAFIA code [5] indicate only low impedance modes in the kicker magnet below the cut-off frequency of the beam pipes. None of these modes were found to be near the potentially dangerous RF system frequency of 500 MHz. Unlike the previous kicker magnets, no damping scheme for resonant modes has needed to be incorporated into the new magnets.

Using the coaxial wire technique [6] a short current pulse was used to model and measure the energy loss from the beam to the kicker magnet. The measurement determines the loss parameter and this was used to estimate the magnet's broadband impedance. A pulse of 20 ps (sigma) was used in the measurement and a loss parameter of 0.70 V/pC obtained. Using an impedance model of a Q=1 resonator centred at the cut-off frequency of the beam pipe (2 GHz) the broadband impedance was estimated as $Z/n = 0.2\ \Omega$. This is an improvement on the impedance of 0.3 Ω for the existing kicker magnets [4].

6. CONCLUSIONS

New compact injection kicker magnets, allowing a redistribution of some lattice elements of the SRS, have been designed, tested and installed. Analytic modelling, finite element analysis and experimental measurements of the magnetic performance agree to first order. A useful reduction in the contribution to the broadband impedance has been achieved.

7. ACKNOWLEDGEMENTS

Thanks are due to S F Hill and L A Welbourne for assisting in the measurements.

8. REFERENCES

[1] Vector Fields Ltd, 24 Bankside, Kidlington, Oxford, UK.
[2] M W Poole et al, Proc. IEEE Part. Accel. Conf., Chicago, 1989, p1250.
[3] M W Poole et al, Proc. EPAC '90, Nice, 1990, p1533.
[4] M W Poole et al, Proc. EPAC '88, Rome, 1988, p830.
[5] T Weiland, Proc. Conf. Computer Codes and the Linear Accelerator Community, Los Alamos LA-11857-C (1990).
[6] M Sands, SLAC Note PEP-95 (1974).